Plate Girders with Corrugated Steel Webs

EZZELDIN YAZEED SAYED-AHMED

Corrugated steel webs were recently proposed to replace the stiffened steel plates of plate/box girders to improve both the aesthetics and the economy of the structure. Girders with corrugated webs are constructed with either steel or reinforced/prestressed concrete (composite) flanges. Composite box-girders with corrugated steel webs are usually prestressed with steel tendons embedded inside the girders. Merits and shortcomings of replacing the conventional webs of plate- or box-girders with corrugated ones are reported elsewhere (Elgaaly, Hamilton, and Seshadri, 1996; El-Metwally and Loov, 1998; Cheyrezy and Combault, 1990; Lebon, 1998; Sayed-Ahmed, 2001).

The web height-to-thickness ratio of corrugated steel webs ranges between 150 and 260 for beams in buildings and may be extended to 450 for bridge girders (Sayed-Ahmed, 2001, 2003): a web height-to-thickness ratio of 445 was recently used for the Hondani Bridge box girder in Japan. Four bridges in France and three in Japan were constructed during the past two decades using girders with corrugated webs (Cheyrezy and Combault, 1990; Combault, Lebon, and Pei, 1993; Naito and Hattori, 1994; Reinhard, 1994; Capra and Leville, 1996; Lebon, 1998; Combault, 1988; Sayed-Ahmed, 2003). Two combined new innovations were used in these bridges: corrugated steel webs and external prestressing. These two innovations are pronounced in the Hondani Bridge (Figure 1) which was completed in Japan in 1998 and in both the Maupré Viaduct and Dole Bridge (Figure 2) which were completed in France in 1987 and 1995 respectively.

The most commonly used corrugation profile for corrugated web plates is the trapezoidal profile for which the main geometric characteristics are shown in Figure 3. It is common for trapezoidal corrugated webs to have the same width for all panels (in other words, a=b and $d/b = \cos \alpha$). Consequently, all the panels will have the same slenderness.

In this paper, the behavior of corrugated steel webs is explicitly investigated. The different buckling modes which may be encountered for these plates are presented and the interaction between these modes is inspected. The interaction between the yield failure criterion and these buckling modes is also investigated. An interaction equation which considers the different failure criteria including steel yielding is then proposed. A linear elastic numerical analysis

Ezzeldin Yazeed Sayed-Ahmed is associate professor, structural engineering department, Ain Shams University, Cairo, Egypt, (on leave to University of Qatar, Civil Engineering Department, Dohar, Qatar).

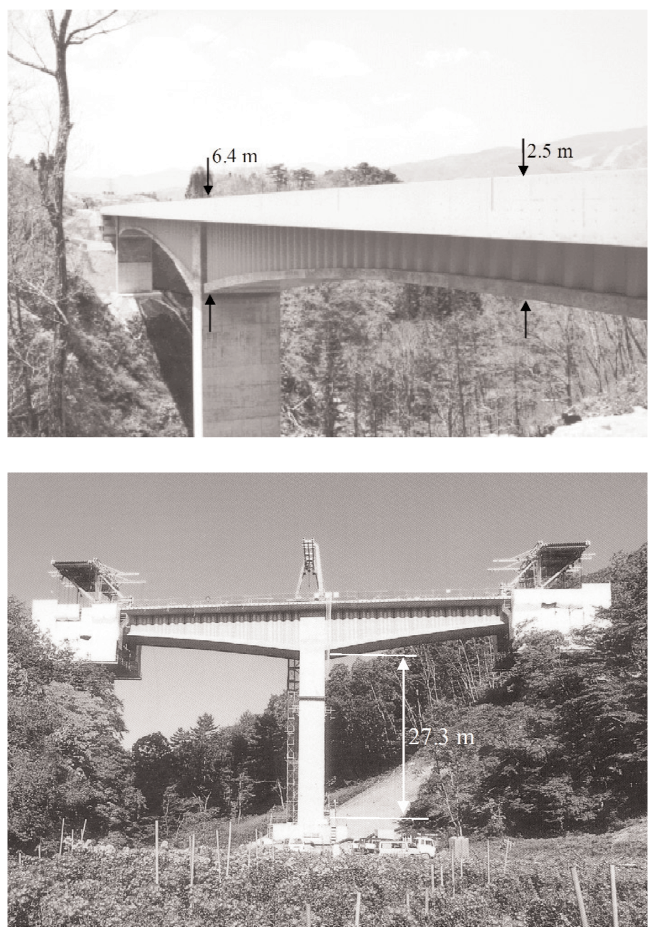

Fig. 1. The Hondani Bridge (Japan) after completion (above) and during construction (below).

which is based on the finite element technique is performed to investigate the buckling modes of the corrugated web plates. A nonlinear finite element model which considers both the geometric and the material nonlinearities is then employed to verify the validity of the proposed interaction equation. The paper scrutinizes the effect of different geometric characteristics of the corrugated webs on their behavior and failure modes. The post-buckling strength of corrugated web girders is also investigated using the nonlinear numerical model.

GENERAL BEHAVIOR OF GIRDERS WITH CORRUGATED WEBS

Flexural strength of a steel girder with a corrugated steel web plate is provided by the flanges with almost no contribution from the web. Furthermore, there is no interaction between flexure and shear behavior of these girders. Thus, the ultimate moment capacity of a steel girder with a corrugated steel web can be based on the flange yield strength (Bergfelt and Leiva-Aravena, 1984; Leiva-Aravena, 1987; Luo and Edlund, 1994; Elgaaly, Seshadri, and Hamilton, 1997; Johnson and Cafolla, 1997). The flexural capacity of composite girders with corrugated steel webs was also investigated and the same aspects defined for steel girders were found to be applicable to composite girders: that is, web contribution to the flexural strength is negligible and there is no interaction between the flexure and the shear behavior (El-Metwally and Loov, 1998, 1999).

The corrugated steel web is assumed to provide the shear capacity of the girder where the shear strength is controlled by buckling and/or shear yielding of the web (Bergfelt and Leiva-Aravena, 1984; Leiva-Aravena, 1987; Elgaaly and others, 1996; Elgaaly and others, 1997; Johnson and Cafolla, 1997; El-Metwally and Loov, 1998, 1999; Sayed-Ahmed, 2001). Thus, the only significant stress which appears in the corrugated web is pure shear stress. The girder's flanges provide boundary supports for the corrugated web, which lie somewhere between a simply-supported and a clamped boundary. The simply-supported assumption for the web boundary is typical for girders with steel flanges while the clamped assumption is typical when the flanges are made of concrete. The concrete flange (slab) is commonly made composite with the corrugated steel web through shear studs that are welded on a steel plate, which

Fig. 2. The Maupré Viaduct (above) and the Dole Bridge (below) in France.

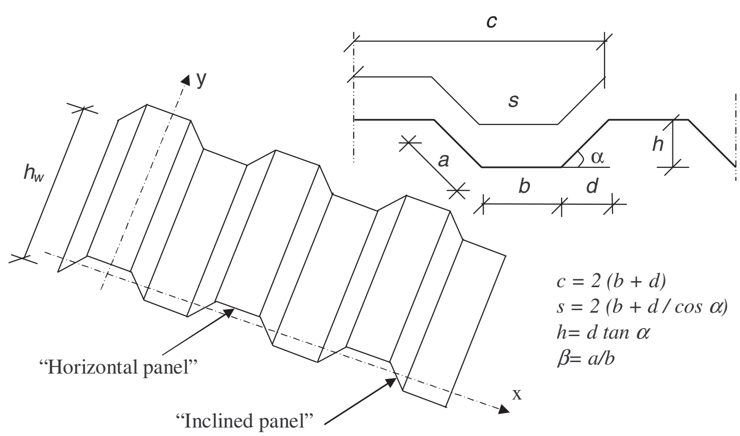

Fig. 3. Trapezoidal profile of the corrugated steel web plates and its geometric characteristics.

is welded to the top of the corrugated web. The shear behavior and the buckling modes of steel girders having corrugated steel webs will be the hub of this paper and will be discussed in detail in the following sections. Plate girders with corrugated steel webs will be considered in all the following analyses. The main concepts which will be derived here are consistently applicable to the corrugated web plates of box-girders (El-Metwally and Loov, 1998, 1999; Sayed-Ahmed, 2001).

FAILURE MODES OF CORRUGATED STEEL WEBS

Failure of a corrugated steel web may occur by shear yielding, buckling or interactively between yielding and buckling.

Steel Yielding of the Web

The shear stress which causes an element of a corrugated web to yield when it is subjected to a pure shear stress state can be determined from the von Mises yield criterion as:

$$\tau_y = \frac{F_y}{\sqrt{3}} \tag{1}$$

where F_y is the yield strength of the steel.

Stability of the Web

Two buckling modes are associated with corrugated steel webs: local buckling and overall (global) buckling. The local buckling mode corresponds to the instability of a steel panel simply supported between two folds. The corrugated web in this mode of failure acts as a series of flat panels that mutually support each other along their vertical (longer) edges. The panels are supported by the flanges along their horizontal (shorter) edges.

Local buckling of a panel between two folds is investigated using equations derived for isotropic plates. Using the theory of stationary potential energy (Galambos, 1998), an estimate for the elastic critical shear stress $\tau_{cr,l}$ for the local buckling mode can be given by:

$$\tau_{cr,l} = k_s \frac{\pi^2 E}{12(1-\upsilon^2)}\left(\frac{t_w}{b}\right)^2 \tag{2}$$

where t_w is the corrugated web plate thickness, b is the panel width, E and υ are the Young's modulus and the Poisson's ratio for the steel respectively and k_s is a shear buckling coefficient for the local buckling mode. The shear buckling coefficient is a function of the boundary restraints and the panel aspect ratio b/h_w with h_w being the web height where:

$$k_s = 5.34 + 4.0\left(\frac{b}{h_w}\right)^2 \tag{3a}$$

$$k_s = 5.34 + 2.31\left(\frac{b}{h_w}\right) - 3.44\left(\frac{b}{h_w}\right)^2 + 8.39\left(\frac{b}{h_w}\right)^3 \tag{3b}$$

Equation 3a is applicable when all the sides of the panels are simply supported which simulates steel girders with corrugated webs. On the other hand, Equation 3b is applicable when the longer sides of the panels are simply supported while the shorter sides are clamped: a typical case for composite girders with corrugated steel webs and concrete flanges.

In Equations 2 and 3, the width of the "horizontal" panel b is used. However, if the "inclined" panel width a is larger than the width of the horizontal panel b, it should be considered as the critical panel width in the previous equations.

Global (overall) buckling is characterized by diagonal buckling over several corrugation panels. The critical shear stress for this mode is estimated by considering the corrugated web as an orthotropic plate. Based on the Ritz method (Galambos, 1998; Easley and McFarland, 1969, 1975), the critical shear stress of this mode $\tau_{cr,g}$ is defined by:

$$\tau_{cr,g} = k_g \frac{\left(D_y D_x^3\right)^{1/4}}{h_w^2 t_w} \tag{4}$$

where k_g is the global shear buckling coefficient which depends solely on the web top and bottom constraints: k_g is 36 for steel girders and 68.4 for composite girders (Elgaaly and others, 1996; Johnston and Cafolla, 1997; Sayed-Ahmed, 2003). The factors D_x and D_y are the flexural stiffness per unit corrugation about the x- and the y-axes respectively (Figure 3). These factors are defined as follows (Galambos, 1998; El-Metwally and Loov, 1999; Sayed-Ahmed, 2001):

$$D_x = \frac{EI_x}{c} = \frac{E}{b+d}\left(\begin{array}{c}\dfrac{bt_w\left[d\ \tan\alpha\right]^2}{4} \\ +\dfrac{t_w\left[d\ \tan\alpha\right]^3}{12\sin\alpha}\end{array}\right) \tag{5a}$$

$$D_y = \left(\frac{c}{s}\right)\left(\frac{Et_w^3}{12}\right) = \left(\frac{b+d}{b+d/\cos\alpha}\right)\left(\frac{Et_w^3}{12}\right) \tag{5b}$$

where I_x is the second moment of area of one "wavelength" of the web having a projected length c and an actual length s, t_w is the web thickness, b is the panel width, d is the horizontal projection of the inclined panel width (Figure 3) and $d \tan \alpha$ is the corrugation depth.

INTERACTION BETWEEN FAILURE MODES

The following equation has been used to account for the interaction between the buckling modes described earlier (Bergfelt and Leiva-Aravena, 1984; Elgaaly and others, 1996; Johnson and Cafolla, 1997):

$$\frac{1}{\tau_{cr,\,i}} = \frac{1}{\tau_{cr,\,l}} + \frac{1}{\tau_{cr,\,g}} \tag{6}$$

where $\tau_{cr,i}$ is the critical stress due to the interaction between local and global buckling modes.

Equation 6 does not consider the steel yielding failure criterion or its interaction with the buckling failure criteria. Furthermore, Equations 2 and 4 do not account for inelastic buckling which occurs if the critical shear stress of any mode exceeds $0.8\tau_y$. To overcome these defects, the following equation was proposed (Elgaaly and others, 1996; Galambos, 1998) for the inelastic critical stress $\tau_{cr,in}$ in both the local and global buckling modes:

$$\begin{aligned} &\text{for } \tau_{cr,l} > 0.8\tau_y : \tau_{cr,in,l} = \sqrt{0.8\tau_{cr,l}\tau_y} \quad \text{where} \quad \tau_{cr,in,l} \le \tau_y \\ &\text{for } \tau_{cr,g} > 0.8\tau_y : \tau_{cr,in,g} = \sqrt{0.8\tau_{cr,g}\tau_y} \quad \text{where} \quad \tau_{cr,in,g} \le \tau_y \end{aligned} \tag{7}$$

To calculate the critical stress for an inelastic interactive buckling mode, the values of $\tau_{cr,in,l}$ and $\tau_{cr,in,g}$ are used in Equation 6 instead of $\tau_{cr,l}$ and $\tau_{cr,g}$ respectively.

Proposed Interaction Equation

Another interaction equation which includes all the failure criteria has been proposed (El-Metwally and Loov, 1999; Sayed-Ahmed, 2001). The new equation takes the form:

$$\left(\frac{1}{\tau_{cr,\,i}}\right)^n = \left(\frac{1}{\tau_{cr,\,l}}\right)^n + \left(\frac{1}{\tau_{cr,\,g}}\right)^n + \left(\frac{1}{\tau_y}\right)^n \tag{8}$$

where τ_y, $\tau_{cr,l}$ and $\tau_{cr,g}$ are defined by Equations 1, 2 and 4, respectively. Equation 8 provides the least value of the 3 limits of the right-hand side as the upper limit for the resulting $\tau_{cr,i}$ in the left-hand side, regardless of the value of the exponent n. A low value for n (for example, n = 1) results in $\tau_{cr,i}$ being considerably less than the least of the three limits. On the other hand, higher values for n will bring $\tau_{cr,i}$ closer to the least of the three limits. The author recommends a value for n of 3.0 which will be valid for most common corrugation profiles (Sayed-Ahmed, 2001).

Typical critical shear stress curves for a trapezoidal corrugated web are plotted in Figure 4. The curves are plotted for girders with steel flanges using the previous equations. Design charts and investigation on the failure modes of these girders are presented elsewhere (Sayed-Ahmed, 2001). It is evident from Figure 4 that, unlike traditional flat webs, the behavior is not uniquely governed by the web height-to-thickness ratio (h_w/t_w). Despite the fact that the same h_w/t_w ratio was used in both graphs of Figure 4, different behavior was recorded for a corrugated web with h_w = 2000 mm (78.740 in.) and t_w = 4 mm (0.158 in.) compared to a web with h_w = 1000 mm (39.370 in.) and t_w = 2 mm (0.079 in.). To neutralize this effect, the critical shear stress curves may be plotted versus the b/h_w ratio rather than versus the panel width b as shown in Figure 5 for h_w/t_w ratios which range between 125 and 500.

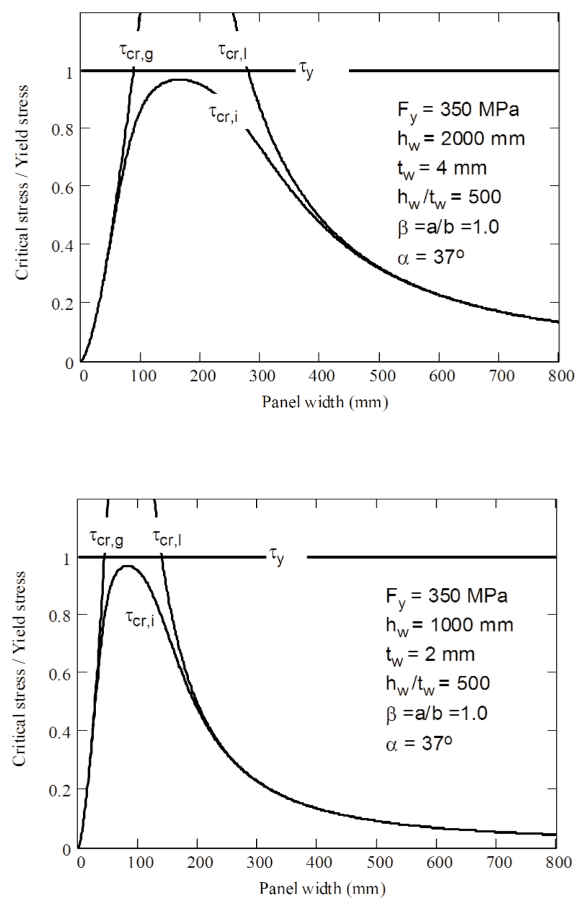

Fig. 4. Critical stresses for trapezoidal corrugated web plates.

Table 1. Dimensions of the Analyzed Steel Girders with Corrugated Steel Web Plates

Girder No.	b	t_w	h_w	b/h_w	h_w/t_w	b_{fl}	t_{fl}	L (span)
	mm (in.)					mm (in.)		m (ft)
G1	400 (15.748)	2 (0.079)	500 (19.685)	0.8	250	300 (11.811)	20 (0.787)	10.48 (34.383)
G2	300 (11.811)	2 (0.079)	500 (19.685)	0.6	250	300 (11.811)	20 (0.787)	7.86 (25.787)
G3	200 (7.874)	2 (0.079)	500 (19.685)	0.4	250	300 (11.811)	20 (0.787)	5.24 (17.192)
G4	100 (3.937)	2 (0.079)	500 (19.685)	0.2	250	150 (5.906)	20 (0.787)	4.06 (13.320)
G5	20 (0.787)	2 (0.079)	500 (19.685)	0.04	250	50 (1.969)	20 (0.787)	2.252 (7.388)

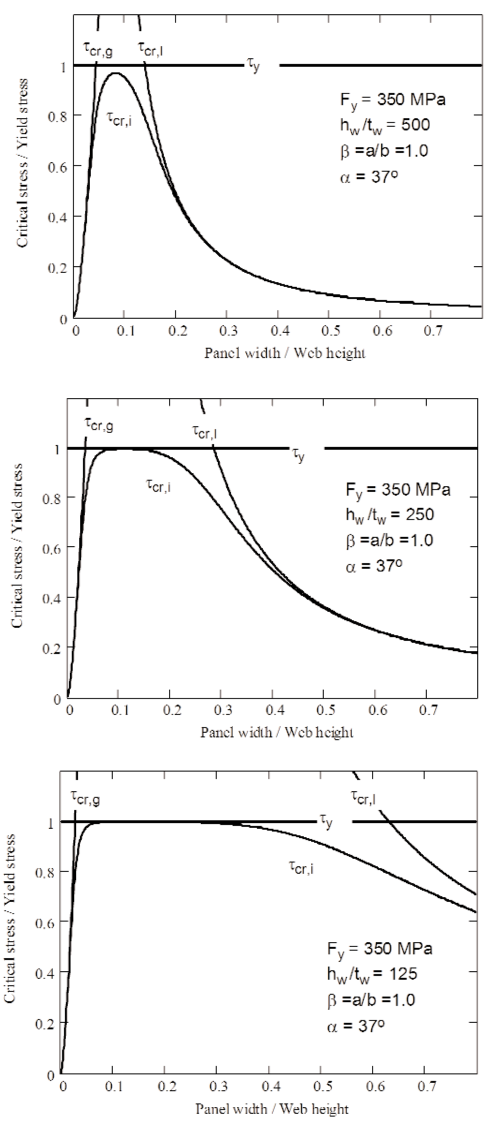

Fig. 5. Behavior of trapezoidal corrugated web plates having different b/h_w *and* h_w/t_w *ratios.*

NUMERICAL MODELLING OF CORRUGATED WEB GIRDERS

Numerical analysis of steel girders with corrugated steel webs was performed using the finite element technique. A linear elastic finite element model was adopted to assess the buckling modes previously discussed, using an Eigenvalue analysis technique. A nonlinear finite element model which considered both the geometric and the material nonlinearities was also developed to investigate the validity of the proposed interaction equation (Equation 8). The nonlinear model was then extended to investigate the post-buckling strength of the corrugated web girders by adopting an arc-length iterative algorithm (Crissfield, 1986) to overcome the snap-through and the snap-back convergence problems associated with the buckling behavior.

Throughout the numerical analyses, isoparametric 8-node shell elements were used to model both the flanges and the corrugated web of the girder. The finite element package ANSYS 5.4 is used for pre-processing of the model data, solution of the finite element equations and post-processing of the analysis results.

The numerical analyses were performed on girders which have 20 mm (0.787 in.) thick steel flanges and a web height-to-thickness ratio of 250. Different panel widths were adopted in the analyses which ranged between 20 mm (0.787 in.) and 400 mm (15.748 in.). These panel widths correspond to panel width to web height ratios ranging between 0.04 and 0.8. The dimensions and the geometric characteristics of the analyzed girders are listed in Table 1. The geometry and loading configurations of these girders are shown in Figure 6 together with the steel uniaxial stress-strain relation adopted in the nonlinear finite element analysis. Stiffener plates 20 mm (0.787 in.) thick were added at the loading and the support locations for all the analyzed girders as shown in Figure 6. The analyzed girders were assumed to be simply supported and were subjected to mid-span concentrated loads (line loads acting on the top flanges as shown in Figure 7). Thus, the shear force acting on the web V is:

$$V = \tau h_w t_w \tag{9}$$

where τ is the shear stress acting on the web.

Due to symmetry, only one half of the girder was analyzed with a plane of symmetry located at the girder centerline. To eliminate the mesh sensitivity effect on the numerical analysis results, the finite element analyses were first performed using different trail meshes having different element sizes. The numerical analyses results obtained using the typical finite element meshes shown in Figure 7 proved to be mesh independent.

The critical load at which web buckling was first encountered during the analysis was determined in both the Eigenvalue linear analysis and the nonlinear analysis. The results of the numerical analyses are plotted in Figure 8 where the

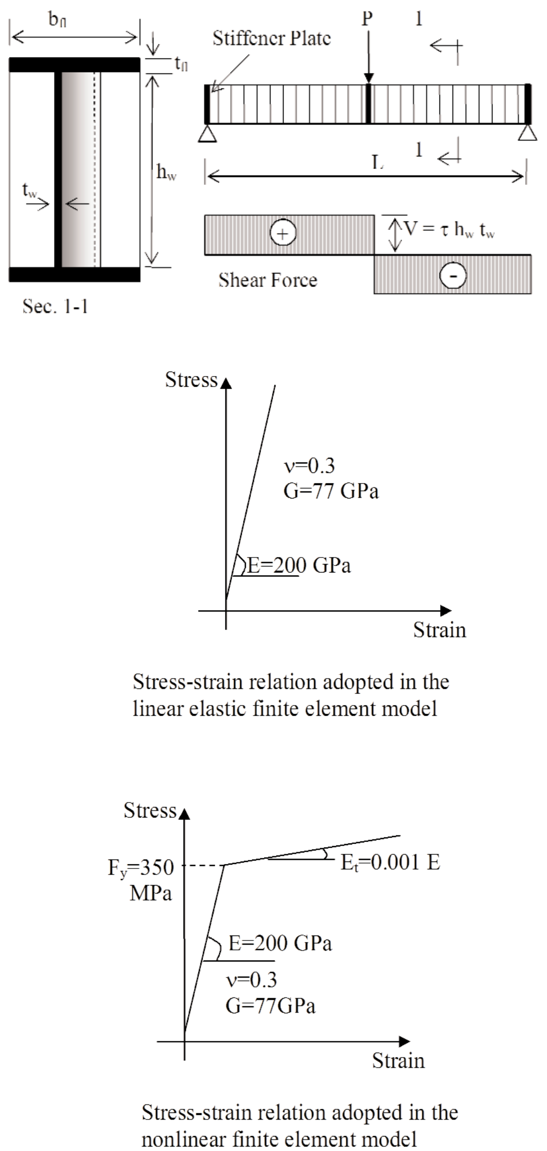

Fig. 6. Geometry, loading configuration and material model adopted in the numerical analyses of the corrugated steel web girders.

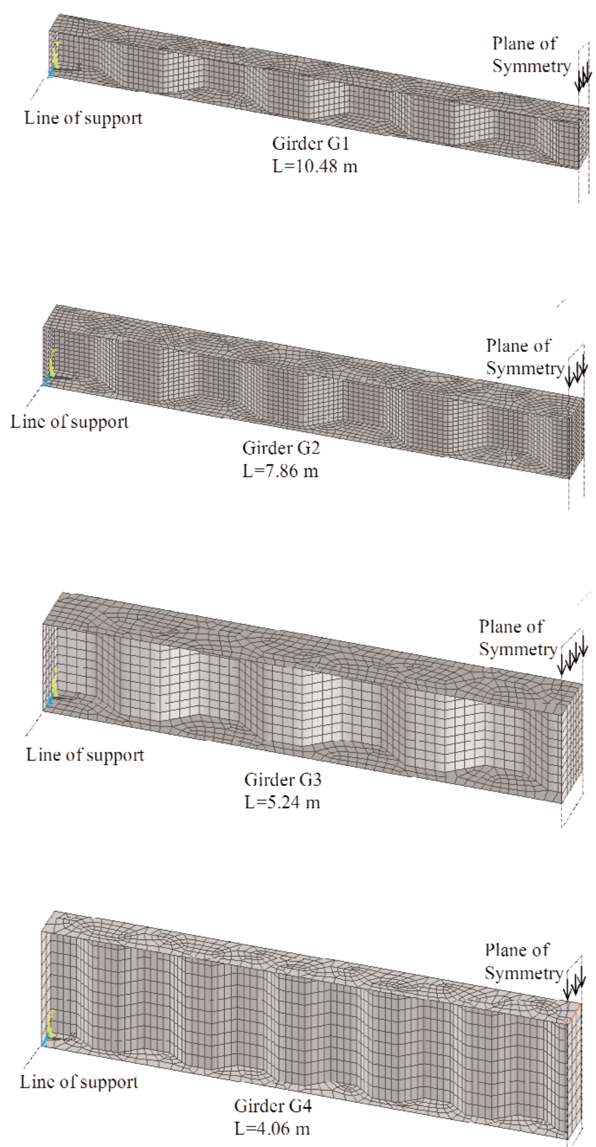

Fig. 7. Finite element meshes adopted in analyzing girders with corrugated steel web plates (girders are plotted with different scales).

ratio between shear force V_{cr} at which web buckling initiated (obtained numerically and using Equations 1 to 8) to the shear force causing steel yielding V_y ($\tau_y\, h_w\, t_w$) is plotted versus the panel width *b*. It is evident from Figure 8 that the results of the numerical analyses are in a good agreement with the behavior theoretically predicted by the proposed interaction equation (Equation 8). Furthermore, the results of the numerical analyses (Figure 8) reveal that Equations 6 and 7 are very conservative compared with the proposed interaction equation. Figure 8 also shows that global buckling governs the behavior for small panel widths (dense corrugation) while local buckling governs it for wider panel widths. Local, global or interactive buckling mode is specified by inspecting the deformed shape resulting from the analysis: Figure 9 shows local and global buckling modes for Girders G3 and G5 respectively. For girders G3, the deformed shapes shown in Figure 9 were obtained from two numerical analyses: one having a finer finite element mesh than the other. The difference in the critical load for the two solutions was less than 1.5 percent. It is also evident from

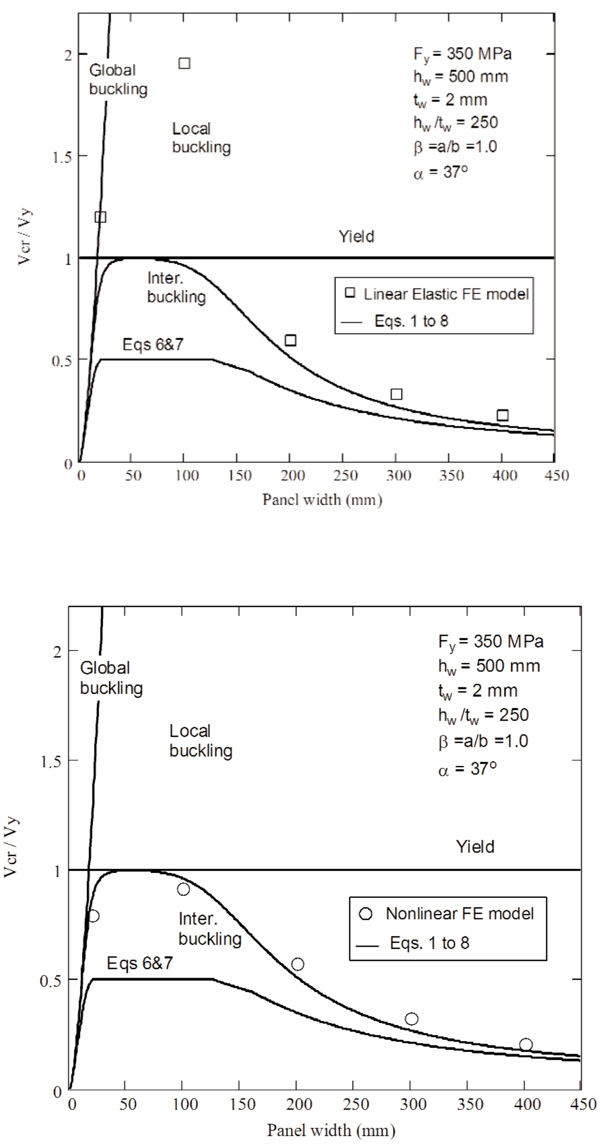

Fig. 8. Critical loads for corrugated web girders determined form Equations 1 to 8 and the numerical models adopted for the linear analysis (above) and the nonlinear analysis (below).

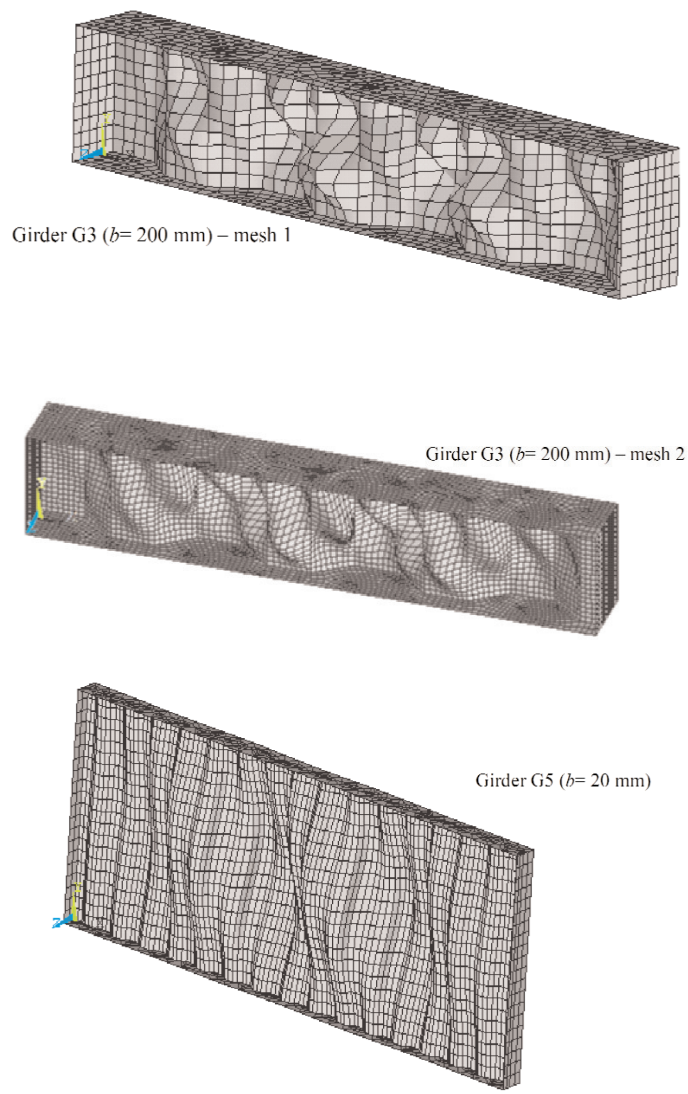

Fig. 9. Local buckling of Girder G3 having a 200 mm (7.874 in.) panel width (above and center) and global buckling of Girder G5 having a 20 mm (0.787 in.) panel width (below).

Figure 9 that failure of Girder G3 occurred by local buckling in the two analyses.

EFFECT OF GEOMETRIC CHARACTERISTICS ON WEB FAILURE MODES

Panel Width Effect

The interaction among the local and global buckling modes and the yield failure criterion for trapezoidal corrugated plates with simply-supported boundaries (steel flanges) is plotted in Figure 10 versus the panel width b. In this figure the same panel width is assumed for both the "horizontal" and the "inclined" panels (in other words, $a = b$); this assumption will be verified later.

It is evident from Figure 10 that global buckling mode governs the instability behavior for significantly small corrugation width b (dense corrugation). On the other hand, the local buckling mode governs the behavior for significantly large values of b. For most of the practical values of the panel width, failure occurs due to an interaction between both the buckling modes and the yield failure criterion.

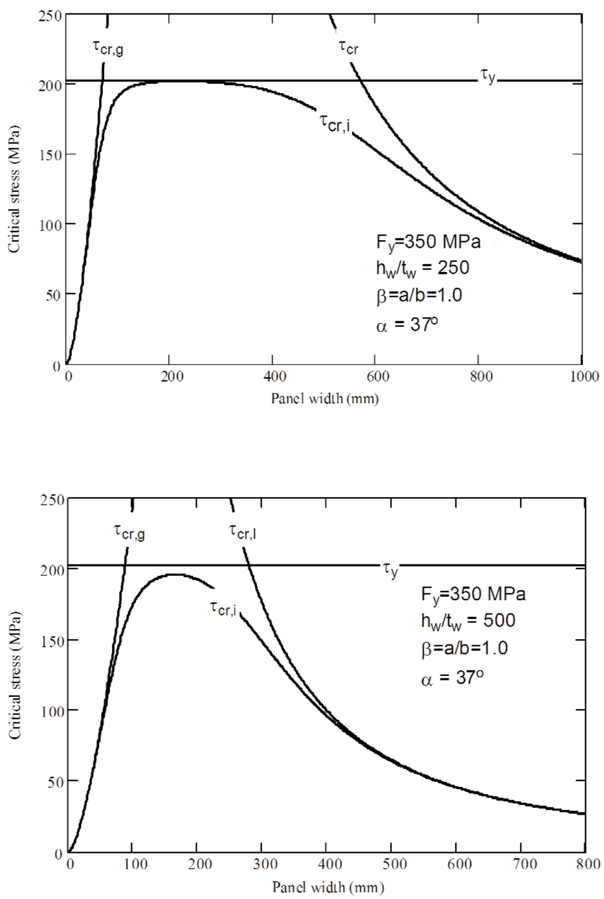

Fig. 10. Interaction between failure criteria for corrugated web plates with h_w/t_w *ratios of 250 (above) and 500 (below).*

Web Height-to-Thickness Ratio (h_w/t_w)

The critical shear stress initiating web buckling for corrugated web girders is plotted in Figure 5 for different web height-to-thickness ratios (h_w/t_w = 125, 250 and 500). A comparison of the behavior shown in Figure 5 reveals that the web height-to-thickness ratio significantly affects the local buckling mode while only slightly affecting the global buckling mode. For higher web height-to-thickness ratios, the local buckling mode governs the behavior for a wider range of the panel width. On the other hand, the global buckling mode is almost unchanged with changing web height-to-thickness ratio (Figures 5 and 10).

Ratio between Inclined to Horizontal Panel Width ($\beta = a/b$)

The ratio between the width of the inclined panel to that of the horizontal panel (defined herein as $\beta = a/b$) has a significant effect on both the local and the global buckling modes. Hence, this ratio also affects the interactive buckling mode. Three β ratios are investigated (β = 0.5, 1 and 2). The results of this investigation are plotted in Figure 11 for the critical stresses resulting from local or global buckling modes and in Figure 12 for the critical stress resulting from an interactive buckling mode.

If the β ratio is less than 1.0 (the horizontal panels are wider than the inclined panels), local buckling occurs in the horizontal panels and governs the behavior. Thus, all the curves which represent the local buckling mode (Figure 11) are identical for β ratios less than 1.0. On the other hand, for a β ratio greater than 1.0 (the inclined panels are wider than the horizontal panels), local buckling occurs in the inclined panels. For a β ratio equal to 1.0, both panels will have the same slenderness and local buckling is equally possible in either panel.

Figure 11 reveals the pronounced effect of the β ratio on the critical stress for the global buckling mode. It is evident from this figure that as the β ratio gets smaller, global buckling controls the behavior for a wider range of the panel width b. This is true because as the inclined panel width gets smaller, and consequently the β ratio gets smaller, the corrugations become denser and hence failure is governed by global buckling through adjacent panels.

The effect of the β ratio on the critical stress resulting from the interactive buckling mode is shown in Figure 12. This figure reveals that the ideal ratio for β is 1.0. At this ratio, the critical stress is close to the yield stress of the steel for a wider range of b. Thus, both the horizontal and the inclined panels are preferably chosen to have the same width.

Effect of the Corrugation Angle

It is evident from Equations 1, 2, 4 and 8 that the corrugation angle α affects neither the yield failure criterion nor the local buckling mode. It only affects the global buckling mode, and thus, it also affects the interactive critical shear stress to some extent. This is also evident from Figure 13 where the critical stress resulting from the interactive buckling mode is only affected by the variation of α in the zone of the global buckling mode.

The interactive critical stress $\tau_{cr,i}$ obtained using Equation 8 is plotted versus the corrugation angle α for different panel widths in Figure 14. It is clear from this figure that the corrugation angle affects the interactive critical stress for small panel widths *b* where the behavior of the corrugated web is governed by either pure global buckling or interaction between global buckling and steel yielding. In Figure 14, the drop that occurs in the critical stress for large panel widths—for example, *b* = 600 mm (23.622 in.)—is mainly due to the effect of local buckling. For such cases, the interactive critical stress $\tau_{cr,i}$ is almost constant through all values of α indicating that the failure occurs by local buckling and is not affected by the change in the corrugation angle.

The effect of the corrugation angle α on the global buckling critical stress $\tau_{cr,g}$ is plotted in Figure 15 for h_w/t_w ratios of 250 and 500. Furthermore, the optimum value of the corrugation angle at which $\tau_{cr,g}$ reaches τ_y is, then, plotted in Figure 16. This figure may be used in design and/or dimensioning of the corrugated web plate to determine the optimum corrugation angle corresponding to a certain pre-specified panel width *b*.

3-D Presentation of the Failure Modes

The failure mode for a corrugated steel web plate is presented in 3-D versus the web height h_w and the panel width *b* in Figure 17. Equation 8 is used to determine the value of the interactive critical stress with the parameter *n* equal to 3.

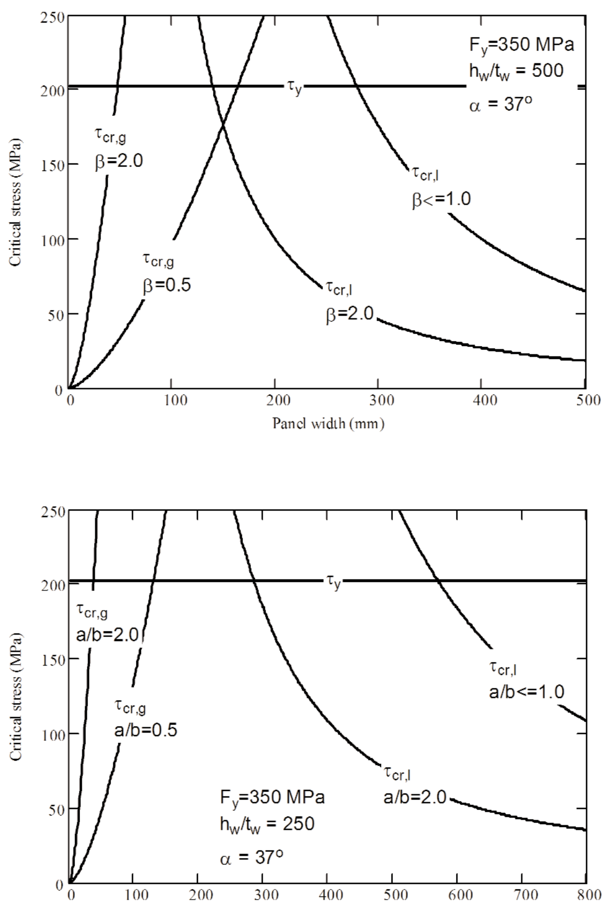

Fig. 11. Effect of the β ratio on the critical stress of the local and global buckling modes for h_w/t_w *ratios of 500 (above) and 250 (below).*

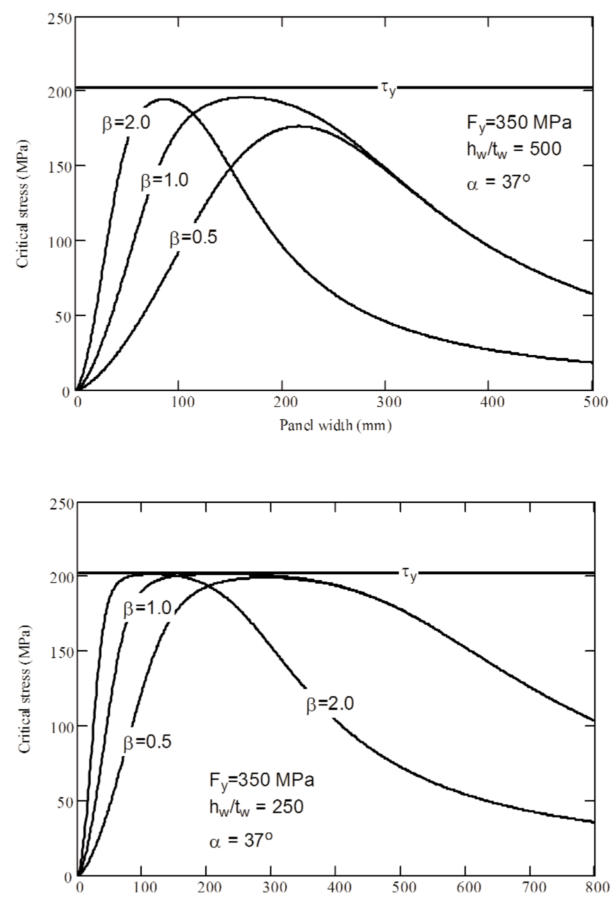

Fig. 12. Effect of the β ratio on the critical stress of the interactive buckling mode for h_w/t_w *ratios of 500 (above) and 250 (below).*

It can be seen from this figure that steel yielding only occurs for small values of h_w. For deeper webs, interaction between yielding and buckling governs the failure criteria. The buckling mode also depends on the panel width as mentioned earlier: panels with small widths exhibit global buckling while larger panels exhibit local buckling.

POST-BUCKLING STRENGTH OF CORRUGATED WEB GIRDERS

The nonlinear finite element model was extended to investigate the post-buckling strength (if any) of corrugated web girders. To overcome the numerical difficulty associated with the buckling behavior, an arc-length iterative algorithm (Crissfield, 1986) was adopted for the incremental iterative procedures.

The numerical analysis reveals that girders with corrugated steel webs continue to carry loads after web buckling is encountered. Hence, the ultimate strength (the load causing final failure) of the corrugated web girders was determined numerically. The critical shear force V_{cr} at which web buckling was first encountered (determined earlier) and the ultimate shear force V_{ult} at which final failure occurred are plotted in Figure 18 versus the web panel width. The percentage of the post-buckling strength $(V_{ult} - V_{cr}) / V_{ult}$ is also plotted in Figure 18.

It is evident from Figure 18 that the post-buckling strength of corrugated web girders is highly dependent on the panel width. For corrugated webs with larger panel widths (which suffer local buckling), the post-buckling strength may reach 53 percent for a 400 mm panel width. On the other hand, for webs with smaller panel widths, particularly those suffering global buckling, the post buckling strength is not significant.

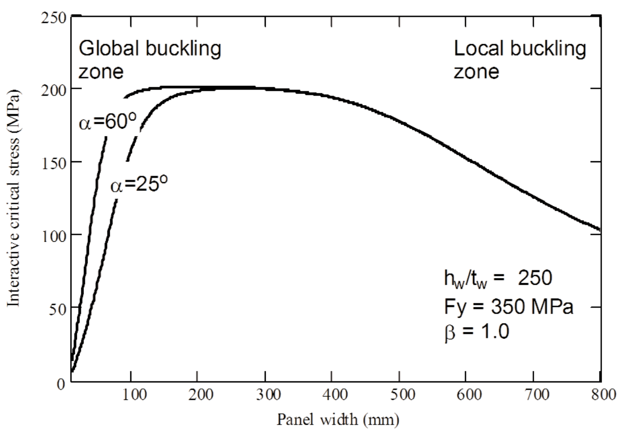

Fig. 13. Effect of the corrugation angle on the interactive critical stress.

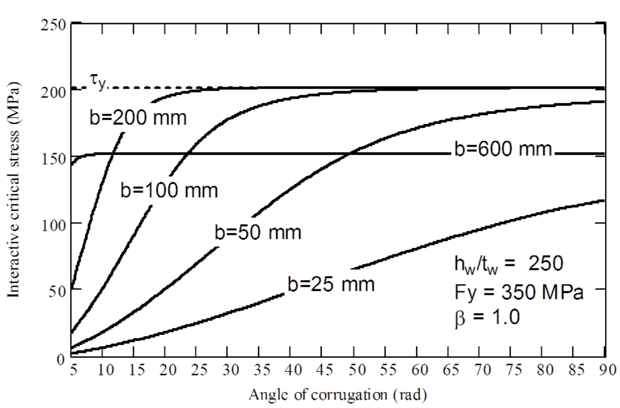

Fig. 14. Effect of the corrugation angle on the interactive critical stress for different panel widths.

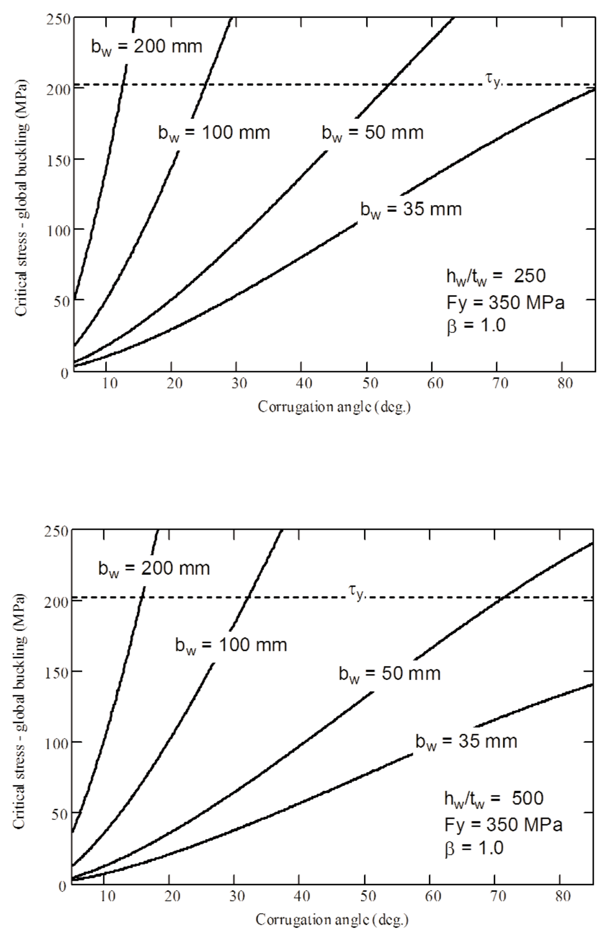

Fig. 15. Effect of the corrugation angle on the global buckling critical stress for h_w/t_w *ratios of 250 (above) and 500 (below).*

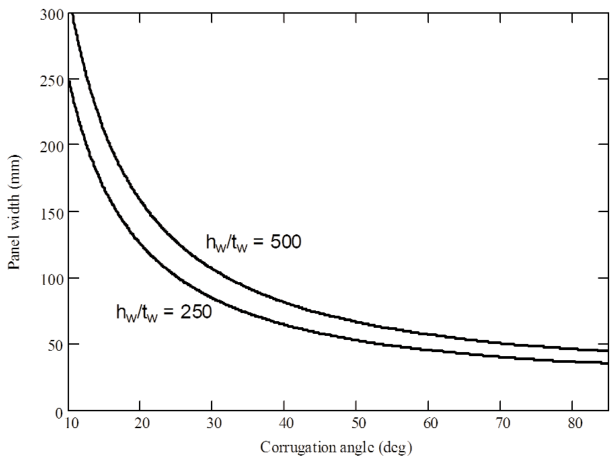

Fig. 16. Corrugation angle versus the panel width at which $\tau_{cr,g} = \tau_y$.

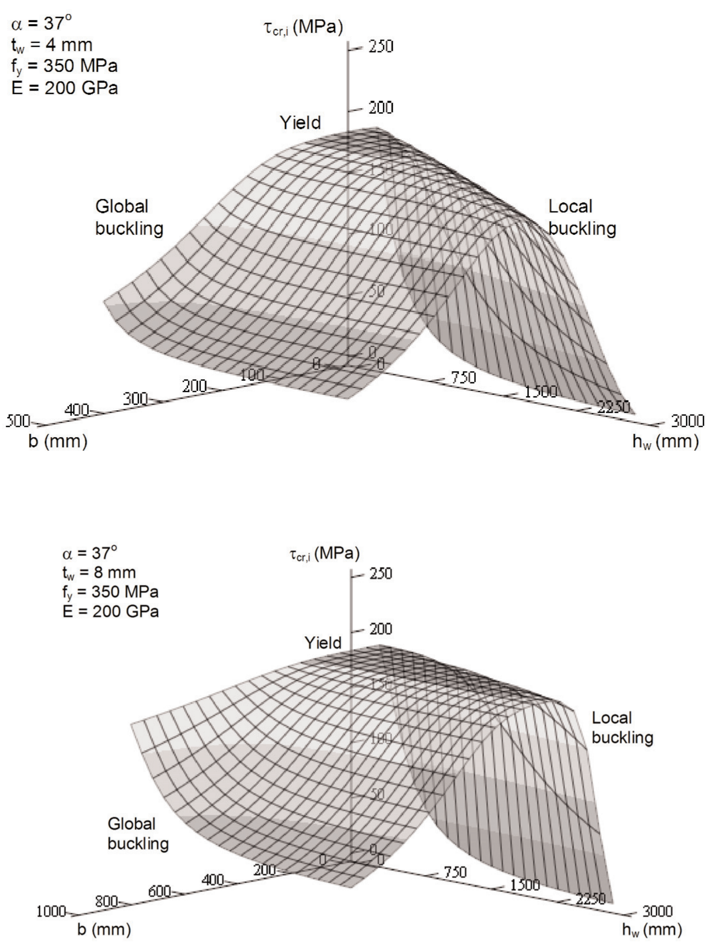

Fig. 17. 3-D presentation of the failure surface for corrugated steel web plates.

SUMMARY AND CONCLUSIONS

Girders with corrugated steel webs have been recently used for different bridges with a height-to-thickness ratio of the web reaching 450. The flexural behavior of the girders is distinct as the corrugated web is assumed to provide only the girder shear capacity with no contribution to the moment capacity of the cross section. It is also evident that there is no interaction between the flexural and shear behavior of corrugated web girders.

The corrugated steel web is subjected to a nearly pure shear stress state. Its behavior is controlled by shear buck-

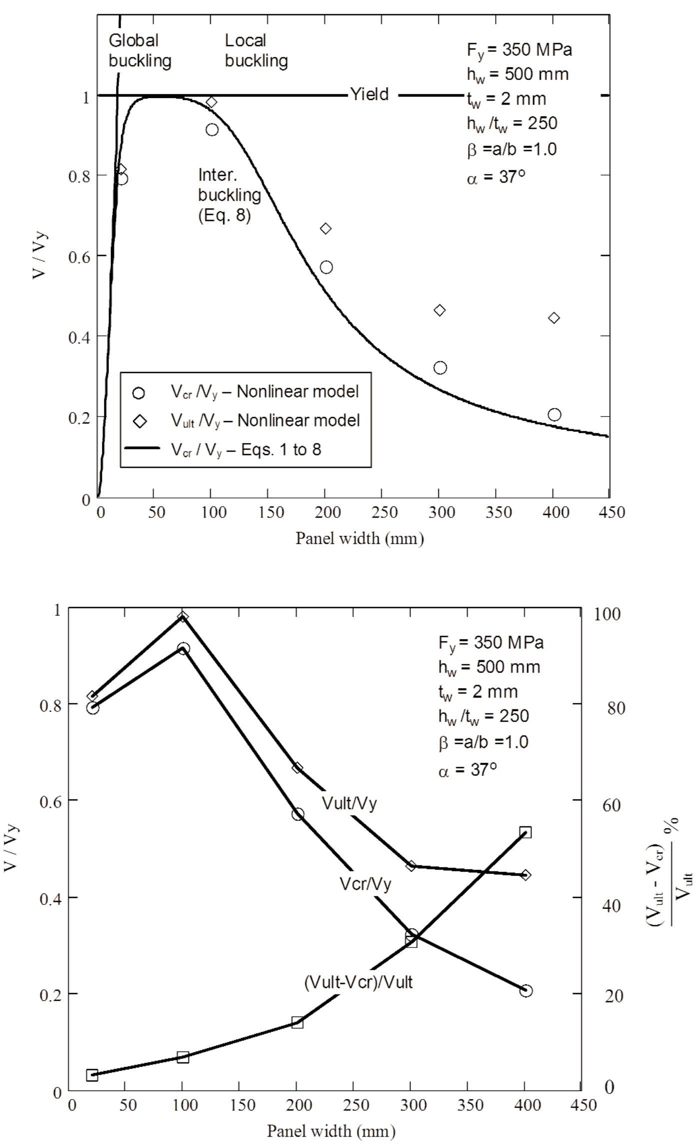

Fig. 18. Post-buckling strength of corrugated web girders.

ling. Two modes of buckling are defined for these webs: local buckling and global buckling. The critical shear stress for local buckling may be determined using the classical isotropic plate theory. On the other hand, the critical shear stress for global buckling is obtained using orthotropic plate equations. An interaction between the local and global buckling modes represents another possibility of failure. Interaction between the different buckling modes and the yield failure criterion of the steel controls the failure of these web plates within all practical ranges of their geometric dimensions.

An interaction equation which defines the interactive failure mode of corrugated steel web plates is proposed. Linear and nonlinear numerical models have been developed to investigate the buckling behavior of corrugated web plates and to examine the validity of the proposed interaction equation. The results obtained from the numerical analyses were found to be in a good agreement with the theoretical prediction obtained using the critical stress equations and the proposed interaction equations. The proposed interaction equation was then used to investigate the effect of the corrugated plate geometric characteristics on its failure mode. The nonlinear numerical model was also extended to inspect the existence of a post-buckling strength for corrugated steel web girders.

It was found that the panel width had the most significant effect on the mode of buckling. An ideal ratio between the inclined panel width and the horizontal panel width for a trapezoidal corrugation profile is proposed to be 1.0. The corrugation angle was found to affect only the global buckling mode and hence the interactive mode to some extent. A design chart for choosing the optimum value of corrugation angle corresponding to any panel width was introduced.

The existence of a post-buckling strength for corrugated web girders was established using the results of the numerical model. However, this post-buckling strength was found to be highly dependent on the panel width of the corrugated webs: the post buckling strength varied between 3 and 53 percent depending on the panel width.

LIST OF SYMBOLS:

a,b	corrugation panel widths
c	projected length of one corrugation 'wave'
d	horizontal projection of the inclined corrugation panel width
E	Young's modulus of the steel
G	shear modulus of the steel
h_w	web height
F_y	yield stress of the steel
k_g	global buckling mode coefficient
k_s	local buckling mode coefficient
I_x	second moment of area of one corrugation wave
s	corrugation amplitude
t_w	thickness of the web plate
V	shear force acting on the corrugated web
V_{cr}	critical shear force initiating web buckling
V_{ult}	ultimate shear force at failure
V_y	shear force causing the corrugated web to yield
α	corrugation angle
β	ratio between horizontal to inclined panel widths of a corrugated web plate
ν	Poisson's ratio
τ_y	yield stress of steel under pure shear stress state
$\tau_{cr,g}$	critical shear stress in a global buckling mode
$\tau_{cr,i}$	critical shear stress in an interactive mode
$\tau_{cr,in}$	inelastic critical shear stress
$\tau_{cr,in,l}$	inelastic critical shear stress in a local buckling mode
$\tau_{cr,in,g}$	inelastic critical shear stress in a global buckling mode
$\tau_{cr,l}$	critical shear stress in a local buckling mode

REFERENCES

ANSYS, Inc. (1997), ANSYS Release 5.4, SAS IP, USA.

Bergfelt, A. and Leiva-Aravena, L. (1984), "Shear Buckling of Trapezoidal Corrugated Girder Webs," Division of Steel and Timber Structures, Chalmers University of Technology, Gothenburg, Publication S 84:2, Sweden, 64p.

Capra, A. and Leville, A. (1996), "The Bridge at Dole," *Proceedings of the FIP Symposium*, Post-Tensioned Concrete Structures. London, Vol. 1, pp. 135-141.

Cheyrezy, M. and Combault, J. (1990), "Composite Bridges with Corrugated Steel Webs—Achievement and Prospects," IABSE Symposium, Mixed Structures: Including New Materials, IABSE Reports, Brussels, pp.479-484.

Combault, J. (1988), "The Maupré Viaduct Near Charolles, France," *Proceedings of the NEC/COP National Steel Construction Conference*, Miami Beach, USA, pp.12.1-12.22.

Combault, J., Lebon, J.D. and Pei, G. (1993), "Box girders using Corrugated Steel Webs and Balanced Cantilever Construction," *Proceedings of the FIP Symposium,* Kyoto, pp. 417-424.

Crissfield, M.A. (1986), "Snap through and snap back response on concrete structures and danger of under integration," *International Journal of Numerical Methods in Engineering*, Vol. 22, pp. 751-767.

Easley, J.T. and McFarland, D.E., (1969), "Buckling of Light-gauge Corrugated Metal Shear Diaphragms," *Journal of Structural Engineering*, American Society of Civil Engineers (ASCE), Vol. 95, No. 7, pp. 1497-1516.

Easley, J.T. and McFarland, D.E. (1975), "Buckling Formula for Corrugated Metal Shear Diaphragms," *Journal of Structural Engineering*, American Society of Civil Engineers (ASCE), Vol. 101, No. 7, pp. 1403-1417.

Elgaaly, M., Hamilton, R.W. and Seshadri, A. (1996), "Shear Strength of Beams with Corrugated Webs," *Journal of Structural Engineering*, American Society of Civil Engineers (ASCE), Vol. 122, No. 4, pp. 390-398.

Elgaaly, M., Seshadri, A. and Hamilton, R.W. (1997), "Bending Strength of Steel Beams with Corrugated Webs," J*ournal of Structural Engineering*, American Society of Civil Engineers (ASCE), Vol. 123, No. 6, pp. 772-782.

El-Metwally, A.S. and Loov, R.E. (1998), "Prestressed Composite Girders with Corrugated Steel Webs," *Proceedings of the 5th International Conference on Short and Medium Span Bridges (SMSB V): Developments in Short and Medium Span Bridge Engineering'98*, Calgary, Canada, pp. 1175-1187.

El-Metwally, A.S. and Loov, R.E. (1999), "Composite Prestressed Concrete Beams with Corrugated Webs," *Proceedings of the Annual Conference of the Canadian Society for Civil Engineering (CSCE)*, Regina, Saskatchewan, Canada, Vol. 1, pp. 305-314.

Galambos, T.V. (1998), "Guide to Stability Design Criteria for Metal Structures," 5th ed., John Wiley and Sons, Inc., New York, USA.

Johnson, R.P. and Cafolla, J. (1997), "Corrugated Webs in Plate Girders for Bridges," *Proceedings of the Institution of Civil Engineering*, Structures and Buildings, Vol. 123, pp. 157-164.

Lebon, J. (1998), "Steel Corrugated Web Bridges—First Achievements," *Proceedings of the 5th International Conference on Short and Medium Span Bridges (SMSB V): Developments in Short and Medium Span Bridge Engineering'98*, CSCE, Calgary, Canada, CD-Proceedings.

Leiva-Aravena, L. (1987), "Trapezoidally Corrugated Panels—Buckling Behaviour under Axial Compression and Shear," Division of Steel and Timber Structures, Chalmers University of Technology, Gothenburg, Report S84:2, Sweden, Publication S 87:1.

Luo, R. and Edlund, B. (1994), "Buckling of Trapezoidally Corrugated Panels using Spline Finite Strip Method," *Thin Walled Structures*, Elsevier Science Limited, Vol. 18, pp. 209-240.

Naito, T. and Hattori, M. (1994), "Prestressed Concrete Bridge Using Corrugated Steel Webs—Shinkai Bridge," XII FIP Congress, National Report, Washington DC, pp. 101-104.

Reinhard, J.M. (1994), "Pont de la Corniche," *Ouvrages d'Art*, No. 19, Nov. 1994, pp. 14-19 (in-French).

Sayed-Ahmed, E.Y. (2001), "Behaviour of Steel and/or Composite Girders with Corrugated Steel Webs," *Canadian Journal of Civil Engineering*, Vol. 28, No. 4, pp. 656-672.

Sayed-Ahmed, E.Y. (2003), "Composite Bridges Constructed with Corrugated Steel Web Box Girders," Proceedings, International Symposium—Celebrating Concrete: People and Practice, Symposium 3: Role of Concrete Bridges in Sustainable Development, Theme 1: Innovative concrete Bridges, University of Dundee, Dundee, Scotland Sept. 2003.